Long-Term Assessment of Cardiac and Behavioral Phenotypes in Mice with Chronic Heart Failure

Megan Mc Manus

A Thesis

in

The Department

of

Health, Kinesiology and Applied Physiology

Presented in Partial Fulfillment of the Requirements

of the Degree of Master of Science (Health and Exercise Science) at

Concordia University

Montreal, Quebec, Canada

June 2024

CONCORDIA UNIVERSITY

School of Graduate Studies

This is to certify that the thesis prepared

By: Megan Mc Manus

Entitled: Long-Term Assessment of Cardiac and Behavioral Phenotypes in Mice with Chronic Heart Failure

and submitted in partial fulfillment of the requirements for the degree of

Master of Science (Health and Exercise Science)

complies with the regulations of the University and meets the accepted standards with respect to originality and quality.

Signed by the final Examining Committee:

_____ Chair

Robert Panenic, MA

_____ Examiner

Dr. Robert Kilgour

_____ Examiner

Dr. Konrad Schoettner

_____ Supervisor

Dr. Andreas Bergdahl

Approved by _____ _____

Dr. Nancy St-Onge, Chair of Department

_____2024 _____

Dr. Pascale Sicotte, Dean of Faculty of Arts and Science

ABSTRACT

Long-Term Assessment of Cardiac and Behavioral

Phenotypes in Mice with Chronic Heart Failure

Megan Mc Manus

Introduction: Heart failure patients have a significant depression risk, with two-to-three-times higher possibility compared to the general population (Rustad et al., 2013). Diminished cerebral oxygen supply from reduced perfusion in heart failure may play a role in the development of mood disorders (Mueller et al., 2020). Suffering from both conditions increases hospitalization and mortality rates compared to patients without depression (Celano & Huffman, 2018). New research is needed for better patient outcomes. Previous murine studies induce cardiac impairments acutely (Frey et al. 2014). However, progressively induced heart failure studies assessing behavior over time are lacking.

Objectives: The aims of this study were: 1) to identify specific timepoints where cardiac phenotypes became more pronounced and, 2) to establish a clear link between the severity of cardiac impairments and the expression of depressive symptoms.

Methods: The plan was to gradually induce heart failure using viral vectors to modify the cardiomyocyte circadian clock through the removal of the clock gene brain and muscle ARNT-Like 1 (*Bmal1*) (Young et al. 2014). Cardiac and behavioral phenotypes were assessed using heart function and behavior tests.

Results: Immunoblotting analysis revealed no difference in BMAL1 protein levels in control and knockout animals. Consistent with the inability to cause heart failure, cardiac and behavioral phenotypes tested were not significantly different between control and experimental groups over time ($p > 0.05$).

Conclusion: The heart-brain relationship remains an important research topic. Future experiments should test viral vectors efficiency at larger concentrations and measure differences in BMAL1 protein expression in heart tissue.

AUTHOR CONTRIBUTIONS

Role of co-authors:

Conception and Design: Megan Mc Manus, Amanda Laplante, Konrad Schoettner, Shimon Amir, Andreas Bergdahl

Data Collection: Megan Mc Manus, Amanda Laplante

Data Analysis and Interpretation: Megan Mc Manus, Amanda Laplante

Drafting of the thesis: Megan Mc Manus

Critical revision of the thesis for important intellectual content: Megan Mc Manus, Konrad Schoettner, Andreas Bergdahl

TABLE OF CONTENTS

LIST OF FIGURES

LIST OF TABLES

CHAPTER 1: INTRODUCTION

1.1 Heart failure and depression

Patients with heart failure have significant risk of developing depression, with a two-to-three-times higher possibility compared to the general population (Rustad et al., 2013). The reciprocal relationship between both conditions also makes someone with depression at increased risk of heart failure (Sbolli et al., 2020). Suffering with both diseases increases hospitalization and mortality rates compared to patients with cardiac problems, without depression (Celano & Huffman, 2018). Unfortunately, the classic therapeutic interventions do not show effective reduction of depressive symptoms for individuals with heart disease, suggesting that new research is needed to advance the field. Current studies investigate the relationship between both diseases by inducing the cardiovascular condition acutely in mice and measuring the effects on mood (Frey et al., 2014). However, progressively induced heart failure studies assessing behavior over time are lacking.

1.2 Healthy heart function

To understand the pathology of heart failure, establishing the function of a healthy heart is essential. The heart muscle is responsible for the distribution of blood with vital nutrients and oxygen to the peripheral system. As tissue oxygen demands increase, cardiac adaptations meet these requirements, which include changes in heart rate, contractility, and modifications to peripheral vascular resistance (Delong & Sharma, 2023; Gilbert et al., 2020). The pumping mechanism is controlled by cardiomyocytes that are activated by action potentials from pacemaker cells in the sinoatrial node (Gilbert et al., 2020). The sinoatrial node manages heart rate with the help of the autonomic nervous system (Gordan et al., 2015). Specifically, adrenergic receptors of the sympathetic nervous system play a key role in increasing heart rate to meet larger oxygen

demands of peripheral tissues (Boyette & Manna, n.d.; Gordan et al., 2015). Understanding how the sympathetic nervous system works in cardiovascular function is important because its dysregulation can lead to the progression of diseases such as heart failure.

During hypoxia, the body sustains organ perfusion by adjusting heart rate and systemic vascular resistance (Bruss & Raja, 2024; Delong & Sharma, 2023). This is an important adaptation to understand because for certain diseases like heart failure, the system will compensate by increasing heart rate and vascular resistance in certain areas to enhance the delivery of oxygenated blood to hypoxic tissue (Delong & Sharma, 2023). In situations where peripheral vascular resistance rises, the system maintains stroke volume by elevating heart contractility or by stimulating vasodilation (King & Lowery, 2024; Ledoux et al., 2003). Consequently, the cardiac system works to maintain oxygen supply to peripheral tissues.

1.3 Heart failure

1.3.1 Prevalence

Heart failure, a functional impairment of the cardiac muscle that decreases peripheral tissue perfusion, is a global health concern (Malik et al., 2024). Currently over 64.3 million people are affected by this heart condition, where the prevalence is expected to increase with an aging population (Savarese et al., 2023). This is a concern because the disease puts an extensive burden on health care systems (Savarese et al., 2023). In the case of Canadians, the economic impact alone amounts to 2.8 billion dollars annually (Yan et al., 2023). Research has a critical role in reducing the impact of the disease by increasing the understanding of its symptoms and progression, which can help health care practitioners by improving prevention plans and creating future medications.

1.3.2 Cardiac remodeling in heart failure

Heart failure arises from cardiac remodeling, a process that leads to additional dysfunction (Azevedo et al., 2016). Changes in the organ's morphology or pathophysiology causes impaired cardiac filling or abnormal blood distribution. Heart failure type will depend on cardiac tissue modifications following compensatory mechanisms to a reduced cardiac output. For example, the cardiac remodeling of a failing heart with preserved ejection fraction arises secondary to increased internal pressures. In this case, exaggerated neurohumoral activation and increased left ventricular filling pressure causes structural and physiological changes, while maintaining normal blood distribution (Savarese et al., 2023). To follow, when the cardiovascular disease is accompanied with reduced ejection fraction, remodeling is specific to overloads following long-term increased neurohumoral activation (Mihl et al., 2008; Schwinger, 2021).

1.3.3 Pathophysiology of heart failure

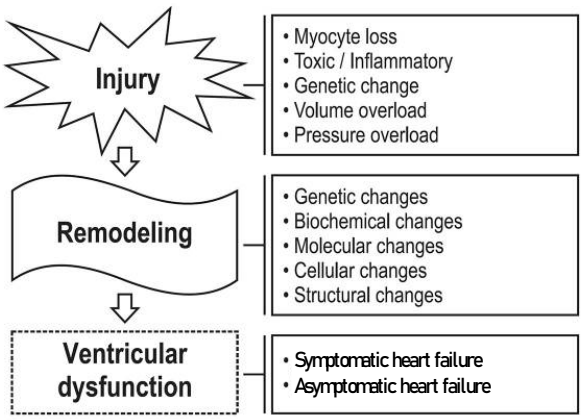

Figure 1: *Ventricle dysfunction in heart failure occurs following physiological or physical changes, where these changes arise following some type of injury to the cardiac tissue (Azevedo et al. 2015)*

The risk of developing different types of heart failure will differ based on factors such as sex, medical history and coexisting cardiac pathologies. Heart failure with preserved ejection fraction is more prevalent in female patients, and is often secondary to atrial fibrillation (Schwinger, 2021). This form of the heart condition is linked to impaired left ventricle filling because of cardiac tissue stiffness (Van Heerebeek & Paulus, 2016). Comparatively, heart failure with reduced ejection fraction is more commonly observed in males as a result of myocardial infarction, sudden high blood pressure, tachyarrhythmias, or heart valve dysfunction (Ge et al., 2019; Regitz-Zagrosek, 2020). Both classifications of heart failure share common risk factors, including aging, chronic hypertension, diabetes mellitus, obesity, and ischemic heart disease (Regitz-Zagrosek, 2020).

When examining the underlying causes of both types of heart failure, a commonality emerges in the form of mechanisms contributing to disease progression. These mechanisms include increased oxidative stress and inflammatory markers, which further injure the cardiac tissue (Iliesiu et al., 2015). The heart works in conjunction with the autonomic nervous system, and a failing heart will prompt adaptations in this neural structure (Gordan et al., 2015). Normally the adrenergic nervous system maintains the cardiac output by stimulating the sympathetic network in stressful situations (Chu et al., 2024). However, prolonged sympathetic activation in a failing heart decreases the adrenergic nervous system's sensitivity and regulation, disrupts heart energy metabolisms, and reduces calcium levels within the cell. These adaptations cause worsening cardiac remodeling and dysfunction (Ge et al., 2019; Lymperopoulos et al., 2013).

In a healthy heart, proper contraction and relaxation is initiated with the release and uptake of calcium ions (Hong & Shaw, 2017). However, patients with heart failure have disturbed calcium

dynamics within the cardiac cells because of T-tubule remodeling, a structure that plays an important role in managing calcium channels (Wei et al., 2010). As a result, impaired calcium transport in the cardiac tissue reduces contraction efficiency, making people more susceptible to arrhythmias and cardiomyocyte death. For instance, tachyarrhythmias can exacerbate heart failure by reducing filling time, consequently decreasing stroke volume and cardiac output (Malik et al., 2024).

1.4 Cardiac function and circadian rhythms

Foundational knowledge about the link between circadian clock function and heart disease will help clarify the process undertaken to induce heart failure in this research project. Although the cardiovascular system is well-equipped to adjust to different oxygen needs over the sleep-wake cycle on its own, the body's circadian rhythm also plays a role in regulating cardiac function. Cyclic regulation of physiological processes, behavior and gene expression is managed by the suprachiasmatic nucleus, the main pacemaker (Zheng et al., 2023). Additional to the main clock, peripheral clocks exist within the cardiac cells and work intrinsically to organise function of endothelial cells, vascular smooth muscle cells, fibroblast, cardiomyocytes, and cardiac progenitor-like cells (Davidson et al., 2005). More specifically, the cardiomyocyte clock first controls ATP generation in preparation for the cardiac contraction phase of the active period. In transition towards the rest phase, the cardiomyocyte circadian clock manages the growth and repair of cardiac cells (Thosar et al., 2018).

Most of the heart rate and blood pressure level rhythmicity is associated with activity levels of dark/light phases. However, the circadian influence, disregarding activity, controls the intensity of the sympathoadrenal and hypertensive responses to stress, causing stronger adaptions during

the awakening phase. The clock's impact is indirect, in line with sympathetic nerves connecting the suprachiasmatic nucleus and the adrenal gland. Therefore, the circadian system helps regulate the magnitude of the variations in heart rate and blood pressure. This was proven by the ablation of *Bmal1* in mice that caused significantly reduced stress responses, regardless of time of day (Curtis et al., 2007). Other evidence of the relationship between cardiac function and circadian rhythm includes cardiovascular event occurrence risk, like myocardial infarction, being time of day dependant (Davidson et al., 2005).

In sum, the coordination between the circadian clock and the autonomic nervous system aids to synchronize heart function in diurnal pattern in preparation for upcoming energy demands of sleep-wake cycles (La Rovere & Christensen, 2015; Wang et al., 2023). This complex rhythmic regulation of heart function emphasizes the critical connection between circadian rhythms and cardiovascular health.

1.5 Clock gene modification and heart disease

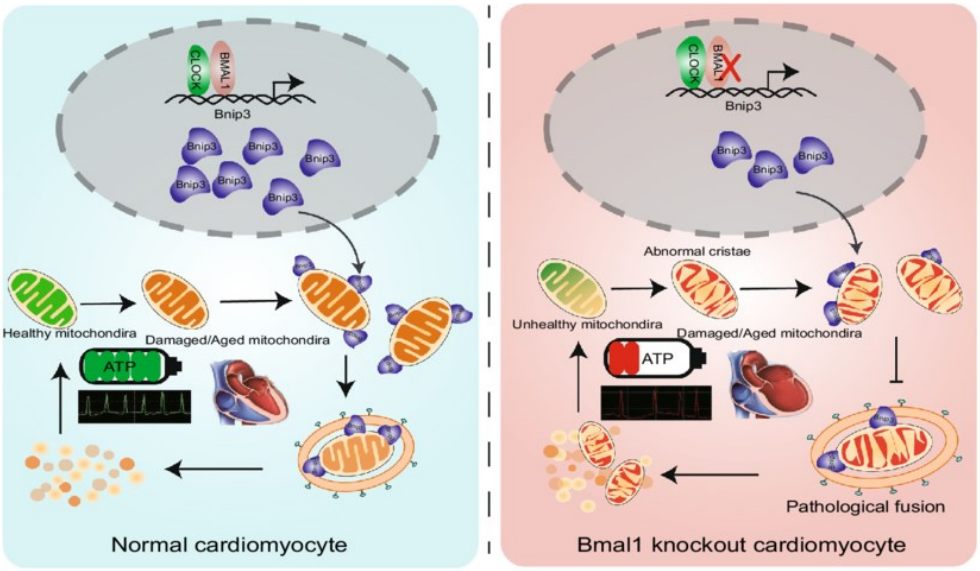

Figure 2: *Bmal1 knockout directly decreases BNIP3 protein levels, a protein that controls the permeability of the mitochondrial membrane. This results in impaired mitophagy and mitochondrial activity and, therefore leads to loss in cardiomyocyte function (Li et al. 2020).*

One of the key regulators of cardiovascular cell circadian rhythmicity is the *Bmal1* clock gene (Crnko et al., 2019). Within heart tissue, this gene is found predominantly in cardiomyocytes, but is also present in vascular smooth muscle cells, endothelial cells, and fibroblasts (Young et al., 2014). Regardless of its presence in other tissues, total *Bmal1* ablation from cardiomyocytes in mutant mice results in severe cardiac dysfunction (Kondratov et al., 2006; Young et al., 2014). This genetic modification impairs mitochondrial function and therefore dysregulates ATP production within cardiomyocytes, leading to further cardiac abnormalities over time (Li et al., 2020). Cardiomyocyte *Bmal1* gene deletion primarily affects rhythmicity within the muscle cells,

while the circadian influence of the primary pacemaker, the suprachiasmatic nucleus, remains intact (Crnko et al., 2019).

In humans, disrupted circadian regulation caused by genetic mutations or lifestyle factors such as irregular sleep patterns or shift work can significantly increase the risk of heart disease (Davidson et al., 2005). This study planned to progressively induce heart failure by removing the *Bmal1* gene using Cre-lox applications for gene modification. This would have represented a chronic heart failure population for researching about the effects of heart disease and depression in mice.

1.6 The Cre-lox applications for altering *Bmal1* gene

Gene manipulation in animals enables research of various pathologies. For a heart dysfunction model, a heart tissue specific *Bmal1* deletion was created using Cre-lox technology. In this system, the enzyme Cre-recombinase recognizes two directly repeated loxP sites in the DNA and inactivates the gene group by excising the genome section (Kim et al., 2018). A conditional knockout can be generated by crossbreeding a "floxed" mouse line with a Cre-driver line. Alternatively, a conditional gene knockout can be generated by injecting adeno-associate viral vectors expressing Cre recombinase (French & Annex, 2014). An adeno-associated virus serotype 9 (AAV9) can be engineered to deliver genes with Cre-recombinase to specific locations. AAV is a protein shell that encapsulates a single stranded DNA genome and serves as the vehicle for genetic material into the system (Naso et al., 2017). To target heart tissue, the viral vectors used can be specific to the gene sequence Cardiac troponin T (cTNT), a cardiac isoform that is exclusively expressed in cardiomyocytes and which is used as a marker of myocardial cell injury. Therefore, a virus can be manufactured to use Cre-recombinase to selectively remove *Bmal1* from

cardiomyocytes through of the AAV delivering to cTNT. Understanding the viral vectors function and its application is essential for determining how the heart dysfunction model can be generated to research behavior in mice.

1.7 Behavioral assessment in animals

Behavioral assessments in animals will be discussed due to the complexity of behavior and the need for careful consideration to ensure reliable evaluation of depressive-like behavior in mice. Tests to assess animals' behavior are made to support that initial thought processes lead to feelings that are associated with healthy or disturbed behavior (DiGiuseppe et al., 2016). Designing the behavioral tests and their analysis requires the consideration of the rodent spontaneous behavior, the animal's motivations, and the influence of the tester (Hånell & Marklund, 2014).

1.7.1 Spontaneous animal behavior

One benefit of assessing this type of behavior is that it alleviates stress induced from performing a task (d'Isa & Gerlai, 2023). However, since this type of testing does not rely on a motivator, a lack of interest to perform the task can be a problem for data acquisition. This problem can be mitigated by longer testing time that allows for larger data sets for analysis (Hånell & Marklund, 2014).

1.7.2 Motivation

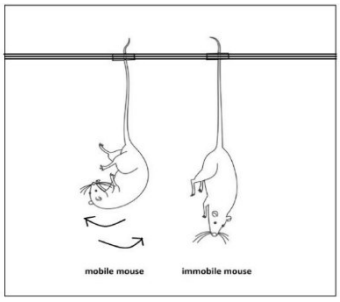

Figure 3: *One example of a valid test that uses fear to motivate for escape is the tail suspension test (Cryan et al., 2005; Hazar-Yavuz et al., n.d.)*

Some behavior tests are designed to provide the maximum motivation for the animal to complete the task to the best of its ability (Hånell & Marklund, 2014). Common motivators are fear to utilize active avoidance learning to stressful stimuli. Fear must be used within the test as a motivator because, if not, it may lead to freezing which may influence cognitive performance (Harrison et al., 2009).

1.7.3 Animal and experimenter interaction

Studies have found that an anxiety-like state in mice modifies exploration behavior and movement, so if the animal is predisposed to any stressful stimuli from the experimenter, this could greatly impact the data. Animal familiarization with the experimenter is important to reduce the stress levels, thus suggesting the importance of handling the mice prior to behavioral experimentation (Segelcke et al., 2023).

1.7.4 Considerations in behavioral analysis

It is essential to be mindful of factors affecting behavioral phenotypes in animals such as the rodent's source of motivation and its natural reactions to stimuli (Belovicova et al., 2017). The test validity is based on these constructs, and monitoring potential behavioral influences during the test is essential to assure that the results are reliable (Hånell & Marklund, 2014).

1.7.5 Assessment of depression in rodents

The complexity of a mood disorder like depression comes from the condition being characterized by several behavioral phenotypes. The multiple emotional symptoms such as despair, anhedonia, self care, and apathy can easily be determined by behavioral tests that have been constructed for animals. However, the animal behavioral analysis has limitations because emotions like worthlessness, guilt and ideas of suicide cannot be measured in rodents (Planchez et al., 2019). The sadness in depression stems from a complex interaction of emotions that cannot be all measures specifically in rodents, therefore the results obtained in behavior tests should be discussed with caution when being compared to complex human behavior (Olbert et al., 2014). Therefore, when looking at depressive-like behavior in animals, it is important to discuss the several behavior phenotypes that can be assessed and make interpretations according to these distinct observations. It is not to be interpreted as depression itself, but only to describe emotional symptoms associated with it.

1.8 Depression and memory

Individuals who are diagnosed with depression demonstrate increased cases of impaired memory recollection compared to healthy adults (Dillon & Pizzagalli, 2018). It is believed that increased stress levels in depression is linked to the reduced ability to consolidate memories. This stress causes the suppression of hippocampal neurogenesis, an important mechanism that mediates pattern separation for recollection of distinct events that are similar. To support this, hippocampus size was compared between depressed and healthy individuals, where volumes were significantly smaller in people with depression (Dillon & Pizzagalli, 2018). Therefore, it is thought that the depressive state is causing the suppression of hippocampal neurogenesis, thus leading to changes in memory formation. Considering this study tested for a depressive phenotype based on the hypothesis that reduced blood flow to the brain causes morphological and physiological changes leading to mood alterations, it included a memory consolidation evaluation for more insight on the mice's mental state.

1.9 Rationale

This project planned to give individuals with cardiovascular disease insight about potential reasons their mental health is degrading following their diagnosis and provide a timeline for depression risk. The complex interactions of the heart and the brain have never been more flagrant, so providing additional foundational knowledge about this relationship furthers the understanding of how depression develops. My project was especially important because it planned to analyse the connection between heart failure and behavioral disorders by examining the extended evolution of associated cardiac and behavioral phenotypes. This research simulated a clinical perspective of how the development of symptoms related to heart failure can influence a person's emotional state.

A mice model was used because we planned to progressively induce heart failure with the deletion of *Bmal1* in cardiomyocytes and observe cardiac and behavioral phenotypes in a controlled environment. Mindful of the translatability of animal research to humans, the information obtained aimed to help health care professionals better understand the progression of these diseases.

This study has significant importance because it addressed the large impact of conditions like heart failure and depression, which can affect anyone. Although the treatment of heart disease has improved immensely in recent years, it remains a persistent health concern. This issue is aggravated by the fact that depression and anxiety are common comorbidities that accompany heart failure, worsening its prognosis. This research topic needed to be addressed because current studies only look at the short-term effects of cardiovascular dysfunction and the development of behavioral phenotypes (Frey et al., 2014). To fill this gap in the literature, my study analysed the long-term relationship between cardiac phenotypes associated with heart disease and the development of behavioral disorders.

1.10 Objectives

1) The primary objective of this research was to identify specific timepoints where cardiac phenotypes become more pronounced. This was to help establish a clear link between the severity of impaired heart function and the expression of depressive symptoms. Specifically, this consisted of thoroughly characterizing cardiac phenotypes as heart failure progressed following the cardiomyocyte-*Bmal1* knockout.

2) The second objective of this study was to assess behavioral phenotypes associated with mood disorders over time following induced heart failure. Understanding how one's mental

state is connected to heart function is essential for tracking the progression of key behavioral abnormalities associated with behavior disorders following heart failure diagnosis.

3) The third objective involved establishing the long-term correlation between the expression of cardiac and depressive phenotypes. This investigation determined if the severity of cardiac symptoms was related to a certain degree of behavioral alterations.

1.11 Hypothesis

We hypothesized that mice with heart failure would show greater cardiac impairment compared to controls. Cardiac dysfunction was expected to manifest in the experimental group as decreased fractional shortening (%) and lower brain perfusion measurements, and a reduced time until exhaustion on the treadmill.

We anticipated cardiac impairments would be associated with increased levels of depressive-like behavior, shown by reduced interest in pleasurable things (anhedonia), heightened levels of anxiety, decreased motivation, and impaired self-care.

Furthermore, when investigating the long-term relationship between the expression of heart failure symptoms and the development of depressive-like phenotypes, we hypothesized that the expression of a depressive-like behavior would worsen as the cardiac impairments became more severe.

CHAPTER 2: EXPERIMENTAL DESIGN

2.0 Methods

This study included 32 *Bmal1* "floxed" mice (Bmal1fl/fl; B6.129S4(Cg)-Arntltm1Weit/J; stock #: 7668, The Jackson Laboratory), with 8 females and 8 males in both control and experimental groups. Animals were screened for any predisposed physiological and behavioral abnormalities/phenotypes. Concordia University's Animal Research Ethics Committee approved all animal methods.

Screening tests	**Included**
Sucrose preference test	Sucrose preference ratio >65% (Mao et al., 2022).
Tail suspension test	Immobility ratio >50% (Steru et al., 1985)
Object recognition test	Recognition ratio >50% (Frey et al. 2014)
Treadmill endurance test	Can maintain a 16.7m/min running speed

Table 1*: Inclusion criteria.*

2.1 Induction of heart failure

At 8-weeks, the cardiomyocyte *Bmal1* knockout (CBK) group received an intravenous injection of cardiotropic viral vectors (AAV9-cTNT-Cre, $1x10^{13}$ vg/ml, 100ul) to remove *Bmal1* specifically in heart muscle cells, provided by PD Dr. Christian Bär (Institute of Molecular and Translational Strategies, Hannover Medical School, Hannover, Germany). The control animals received empty vectors (AAV9-cTNT-empty, $1x10^{13}$ vg/ml, 100ul). A qualitative assessment

using Polymerase Chain Reaction (PCR) of the deletion of *Bmal1* was conducted at the beginning of the study.

2.2 Timeline

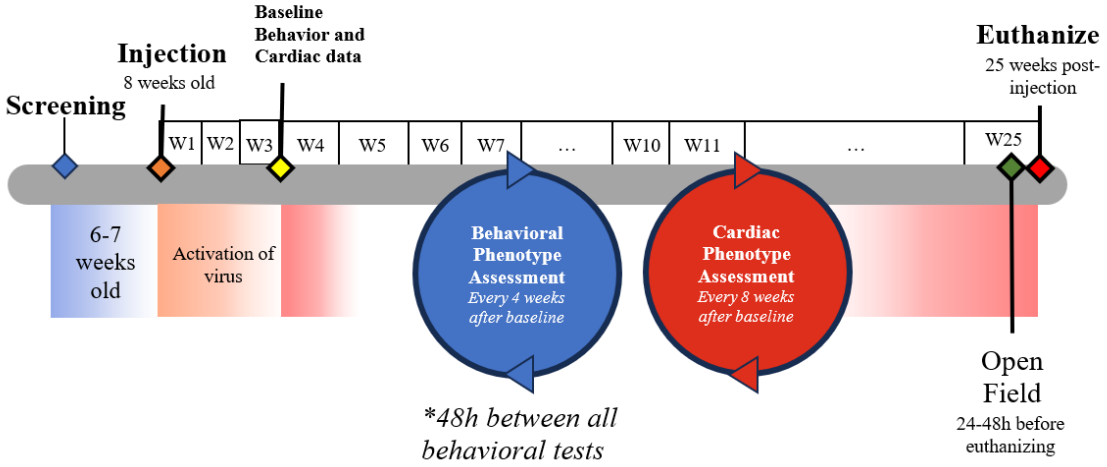

Figure 4: *Timeline of experiment.*

The behavioral test data was collected every 4 weeks and complimented by assessments of cardiac function every 8 weeks. The tissue samples were gathered 25 weeks after the injection. The left ventricle was gathered for mitochondria respirometry. At the end of the study, PCR and Immunoblotting were performed to determine the effectiveness of *Bmal1* deletion in experimental animals.

2.3 Behavioral phenotype assessment

Following the injection, behavioral phenotypes were assessed using the sucrose preference test, splash test, tail suspension test and object recognition test. These tests were conducted with an interval of 48 hours, within 2 to 4 hours after the start of the light phase. The depressive-like

characteristics were identified through the demonstration of increased anhedonia, decreased self-care, diminished motivation, and heightened anxiety-like behaviors.

2.3.1 Sucrose preference test

Assessed the animal's ability to experience pleasure or reward to focus on an important symptom of clinical depression: increased anhedonia. Depressive-like behavior was interpreted by a reduction in sucrose intake compared to water. To minimize the influences of a novel 2 bottle set-up, a habituation period with 2 water bottles was implemented 48 hours before the test. For the test, a sucrose solution bottle (1% sucrose in tap water (w/v)) and a water bottle were provided for 48 hours, switching bottle positions at 24 hours to avoid side preference (Frey et al., 2014). The validity of this method was established in anti-depressive medication studies, where mice exposed to a chronic stress model to induce depressive-like behavior showed increased sucrose preference after receiving anti-depressants, compared to measures taken before treatment (Katz, 1982).

2.3.2 Splash test

An evaluation measuring a key phenotype of depression like self-care habits and motivation through grooming behavior (Planchez et al., 2019). A 10% sucrose solution was sprayed on the back of the mice, and the time from spraying to grooming initiation was measured. Over a 5 minute period, frequency and duration of cleaning bouts was measured, where reduced grooming over time would be suggestive of depressive-like behavior (Bouguiyoud et al., 2022).

2.3.3 Tail suspension test

Evaluated depressive phenotypes like motivation, despair and self-helplessness from measured immobility time when suspended by the tail, on the basis that mice naturally want to escape stressful situations. Immobility time was calculated during 6 minutes of suspension using adhesive tape (Can et al., 2011). The validity of this test was determined by Stukalin et al., (2020), where differences in agitation time were found following delivered anti-depressant medication.

2.3.4 Object recognition test

Measure of short-term memory by assessing novel object compared to familiar object exploration time. Reduced novel exploration compared to the old object suggested poor short-term memory. The mice were put in the open field for 10 min for two sequential habituation days. On day 3, exploration time of 2 identical objects (A1, A2) for 10min (training) was recorded. After 1h, exploration of a familiar object (A2), and a novel object (B) for 10 min (retention) were recorded. Objects were repositioned between trials to account for side preference. A training and retention discrimination ratio (A1/ (A1 + A2) × 100 and B/ (B + A2) × 100) were calculated. An index of over 50% showed the object preference (Frey et al., 2014).

2.3.4 Open field test

Used to measure anxiety-related behavior from general locomotion (Gould et al., 2009). The mice were dropped into an open-field and the distance covered (in cm) during the entire timed portion of the test was measured. Subsequently, the percentage of the total 30-minute test time that the mice spent in the middle of the space was measured. Increased time on the periphery was an indication of anxiety-like behavior because mice have an innate fear of large open areas (Seibenhener & Wooten, 2015)

2.4 Cardiac phenotype assessment

2.4.1 Echocardiography

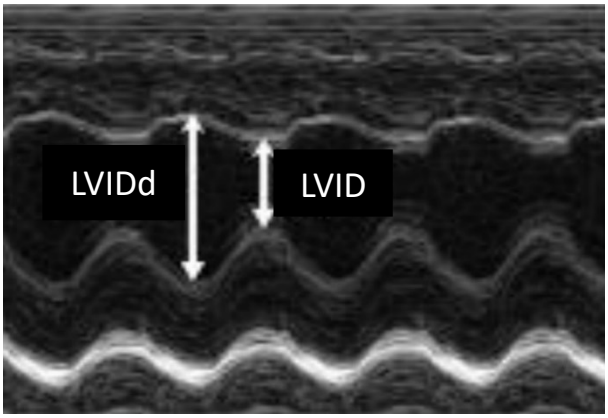

Figure 5*: Ultrasound image of left ventricle M-mode of mice heart (Gao et al. 2011)*

A 13Hz ultrasound probe was used to evaluate left ventricle function in mice anesthetized with isoflurane (2%) (Gao et al., 2011). The evaluation involved observing physical changes using M-mode images, as shown in **Figure 5**, that showed the left ventricular internal dimension during diastole (LVIDd) and systole (LVIDs). To measure cardiac contractility, fractional shortening (FS) (%) was calculated by taking the difference between when the left ventricle internal dimension

was relaxed (LVIDd in **Figure 5**) and when the left ventricle was contracted (LVIDs in **Figure 5**). The value was relative to the relaxed state and then converted into a percentage (**Equation 1**) (Gao et al., 2011).

$$FS\ (\%) = (LVIDd - LVIDs) / LVIDd \times 100 \quad \textbf{(1)}$$

*LVIDd: left ventricle internal diameter during diastole, LVIDs: left ventricle internal diameter during systole (see **Figure 5**)*

2.4.2 Brain fluorescent imaging

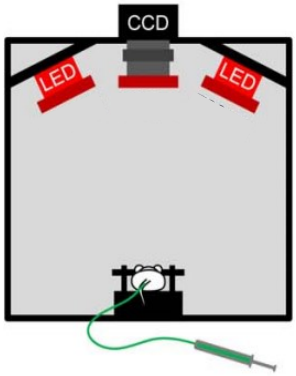

Figure 6: *Brain blood flow set up (Ku & Choi, 2012)*

Fluorescent imaging using intravenous injection of indocyanine green assessed general cerebral perfusion levels to explain changes in the morphology and function of regions regulating mood. Cerebral vascularization was captured with an infrared camera focused on the mice's scalp lit with an infrared light (780 nm) set up as shown in **Figure 6** (Ku & Choi, 2012). This technique was proven to be a sensitive measure of changes in cerebral vascularization by identifying modifications in perfusion as small as differences induced from anesthesia with ketamine compared to isoflurane (Ku & Choi, 2012).

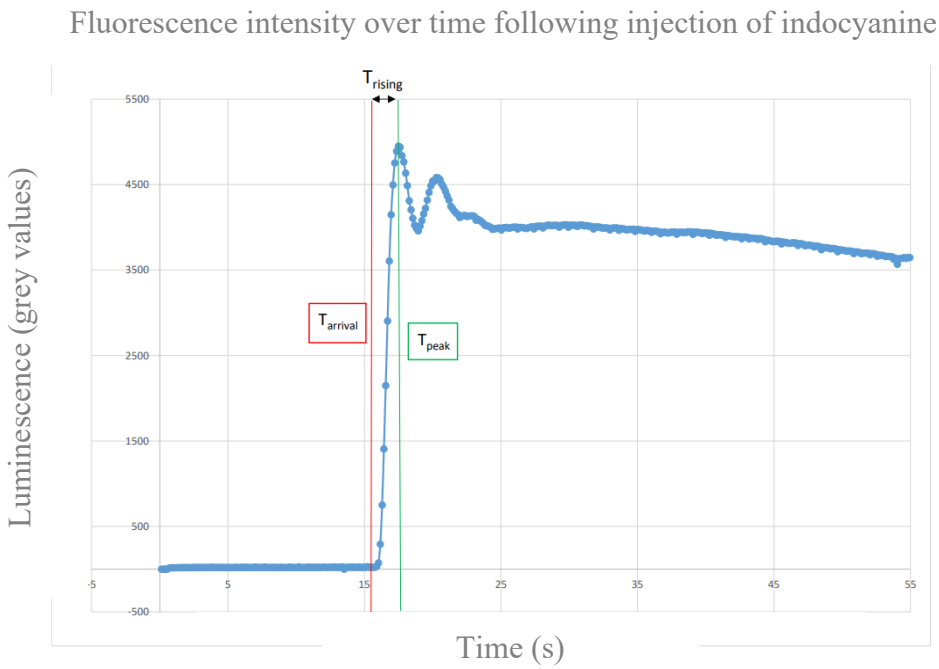

Figure 7: *Small section of indocyanine green dynamics over time following injection, with the arrival time ($T_{arrival}$) and the first peak time (T_{peak}) to calculate the rising time (T_{rising}).*

Local tissue perfusion was measured from the time the fluorescent dye appeared at the brain ($T_{arrival}$) until the peak intensity was reached (T_{peak}), as shown in **Figure 7**. $T_{arrival}$ time was determined as the first frame larger than more that 4 standard deviations of the average of similar intensities in the frames following the injection. Increases in T_{rising} times were an indication of decreased cerebral perfusion. Subsequent peaks following the first peak were caused by systemic recirculation. T_{rising} may be the best measure of cerebral perfusion because it is not affected by the method of bolus delivery (Ku & Choi, 2012).

2.4.3 Rotarod

Used to assess motor coordination and balance by measuring the ability to stay on the rod (Deacon, 2013). Training on the rotarod was conducted for 2 minutes (2 revolutions per minute with rod diameter of 5cm), with mice being placed back on the rod if they fell. Three hours later, mice were put on the rotarod at 2 revolutions per minute for 1 minute, across 3 trials, with 15 seconds rest between each trial. Falls before 5 sec indicated poor placement by the experimenter and the trial was redone. The same protocol was applied for 4, 8, and 12 revolutions per minute, and the time until the mice fall off the rod was calculated for all the trials. The animal's balance score was the average time until failure at each speed. Decreased average time to failure meant lower motor coordination and balance.

2.4.4 Treadmill

***Figure 8**: Mouse treadmill set up.*

A maximum aerobic exercise test was conducted by having the animals run on a treadmill until exhaustion. An acclimatization period consisted of exploring their respective treadmill lane for 2 minutes with the machine off. They ran for 2 minutes at 13.3m/min and 2 minutes at 15m/min as a warm-up. Afterwards, the mice ran at 16.7m/min until exhaustion. Exhaustion was characterized by the mouse no longer sustaining the speed and remaining near the bottom of the treadmill for more than 10 seconds, even following brush stimulation at the end of the track (see **Figure 8**). The time until exhaustion was a measure of maximum aerobic capacity and an indicator of cardiac health.

2.5 Tissue extraction and permeabilization

The mice were euthanized by live decapitation following isoflurane anesthesia. The left ventricle was immediately extracted and permeabilized for mitochondrial respiratory assessment. The isolated tissue was incubated for 30 minutes on ice in 50 µg/mL saponin and 2mL BIOPS

buffer solution [2.77mM CaK2EGTA, 7.23mM K2EGTA, 5.77mM Na2ATP, 6.56mM MgCl2×6H2O, 20mM Taurine, 15mM Na2Phosphocreatine, 20mM Imidazole, 0.5mM Dithiothreitol, 50mM MES (pH 7.1) (Fontana-Ayoub et al., 2013). After, the tissue was washed twice consecutively for 10-minute in MiR05 buffer [0.5mM EGTA, 3.0mM MgCl2×6H2O, 60mM K-lactonionate, 20mM Taurine, 10mM KH2PO4, 20mM HEPES, 110mM Sucrose, 1g/L BSA (pH 7.1)] (Kuznetsov et al., 2008).

2.6 Mitochondrial oxygen consumption

Mitochondrial oxygen consumption was measured via high-resolution respirometry (Oxygraph2k, Oroboros Instruments, Innsbruck, Austria). Approximately 1.0-1.8 mg of heart tissue was added to 2mL of MiR05 buffer in each chamber. The chamber (37°C) was a hyper-oxygenated environment to prevent oxygen limitation. Malate (2mM), glutamate (10 mM) and pyruvate (6 mM) were added sequentially to stimulate LEAK respiration across complex I and to build the proton gradient across the inner mitochondrial membrane. ADP (5mM) was incorporated to initiate complex I-dependent respiration. Cytochrome c (10μM) was added to assess outer mitochondrial membrane integrity. Succinate (10mM) was then added to measure maximal respiration, followed by oligomycin (2μg/mL) to inhibit ATP synthase, and observe maximal LEAK respiration. Lastly, an FCCP (0.25μM) titration was carried out to assess maximal uncoupled respiration.

2.7 Heart weight/Body weight ratio

The final body weight was taken just before euthanasia (g). After, hearts were extracted, drained of blood, and weighed (mg). Heart weight was divided by body weight (g) for this ratio as an indication of cardiac hypertrophy resulting from impaired heart function (Jia et al., 2018).

2.8 Polymerase Chain Reaction (PCR)

PCR amplifies DNA fragments to identify specific gene sequences according to their weight and charge (Garibyan & Avashia, 2013). This technique was used to identify the genetic deletion of *Bmal1* in the heart following the injection of the viral vectors (AAV9-cTNT-Cre). To initially validate the CBK model, a qualitative analysis of gene expression using PCR was performed to identify the "floxed" allele that enables the knockout and identify the sequence confirming the excised *Bmal1* gene. Firstly, the apex of the heart was homogenized, and the cell wall was broken down in NaOH (50MM) heated for 30min at 95°C and then stabilized with TRIS buffer. The solutions were centrifuged at 13 300 rpm for 7 minutes to separate tissue fragments from the solution. To determine if the *Bmal1* sequence had been removed in the heart tissue, loxP/WT/Excision primers were used (0.5uL Bmal1_EX2 L1, 0.5uL Bmal1_EX2 R1 (R), 0.5uL Bmal1_EX2 L2, 12.5uL Mastermix, 9.5uL dH_20). 2uL of DNA was added from each sample separately. Subsequently, to confirm that the Cre component of the virus was present, we used iCre primers (0.5 uL iCre (F), 0.5uL iCre (R), 12.5uL Mastermix, 9.5uL dH_20). The DNA was replicated in the thermocycler. Following the duplication of the DNA sequence, the samples were passed through a 1.5% agarose gel (0.005% ethium bromide) at 100V for 40min. The gel was imaged using the *Kodak system*.

Bmal1_EX2 L1 (Forward primer): ACTGGAAGTAACTTTATCAAACTG

Bmal1_EX2 R1 (Reverse primer): CTGACCAACTTGCTAACAATTA

Bmal1_EX2 L2 (Forward primer): CTCCTAACTTGGTTTTTGTCTGT

iCre Forward: 5'-AGATGCCAGGACATCAGGAACCTG -3'

iCre Reverse: 5'-ATCAGCCACACCAGACACAGAGATC -3'

2.9 Immunoblotting protocol

Considering that genes serve to specify sequences of amino acids, and proteins are responsible for carrying out every function of the cell, to validate the CBK model, we also measured BMAL1 protein expression in heart tissue (Koussounadis et al., 2015). This qualitative analysis of BMAL1 protein expression in heart tissue was done using an Immunoblotting technique. The heart cells were lysed in a NP40 protein detergent containing 1% Nonidet P40, 0,1% of Sodium dodecyl sulfate, 50 mM of Tris, 0,1 mM Ethylenediaminetetraacetic acid, 0,1 mM Egtazic acid and 0,1% deoxycholic acid, pH 7,4. An inhibitor solution made of sodium pyrophosphate 1mM, of sodium orthovanadate 46 1mM, 20mM of NaF, an inhibitor of protease and phosphatase inhibitor (Sigma-Aldrich, P5726-1ML) at 1mM was added to the protein detergent. The lysis was incubated under rotation for 30min at 4°C. The proteins were taken from the supernatant following centrifugation at 13 300 rpm for 10 minutes at 4°C. Protein quantification was done using the pierce bovine serum albumin analysis kit (ThermoScientific, #23227) with the standard curve of Bovine serum albumin from 0-1 ug/uL to obtain a specific protein concentration of 30ug. The protein was mixed with protein loading detergent Laemmli 4X (Bio-Rad, #1610747) in a 60uL total volume heated at 95°C for 5min to denature the proteins. The

protein samples were separated with a polyacrylamide electrophoresis gel in presence of Sodium dodecyl sulfate on a 10% acrylamide gel using a Mini-PROTEAN Tetra System (Bio-Rad). Protein migration was performed in an electrophoresis solution 1X Tris-Glycine for 30min at 100V to bring the proteins together, then 1h at 120V for the migration in the separation gel. Under cold conditions, the proteins were transferred on to a 0.2 µm nitrocellulose membrane (Bio-Rad, #1620112) for 1h at 100V in a transfer detergent 1X TrisGlycine-methanol. The membrane was then blocked in Tris-saline buffer-Tween-Bovine serum albumin at 5% for 1h at room temperature. The blocked membrane was incubated at 4°C with the primary antibody until the next day before being incubated with the secondary BMAL1 antibody (B-1) (Novus Biologicals, # NB100-2288, Littleton, CO, USA, 1:1000) for 1h at room temperature. The proteins were detected using the Clarity Western ECL Substrate (Bio-Rad, #170-5061). The density of the immunoblots was analysed using ImageJ software (*Fiji Software*).

CHAPTER 3: RESULTS

3.0 Results

3.1 Validation of viral vectors (AAV9-cTNT-Cre) function using PCR

To validate the CBK model, a qualitative analysis of gene expression in heart tissue using PCR was performed to identify the DNA sequence with excised *Bmal1*, and the paired loxP sites that enables the knockout (*Bmal1* floxed animals, lox/lox). Ear tissue was used as a control. A heterozygote lox/+ animal was also used as a control, where a lack of paired loxP sites was confirmed by a 327 bp band and a 431 bp band in the heart and ear tissue. To follow, homozygote lox/lox genotype was confirmed in control and experimental animals' heart and ear tissue that expressed a single 431 bp band. Finally, only the knockout animals had a second ~580 bp band from heart tissue samples, representing the knockout product (**Figure 9A**). The knockout was only seen in the heart tissue, confirmed by ear tissue samples that only showed a single 431 bp band. This demonstrated that the *Bmal1* in ear tissue was unaffected in CBK mice. Cre was only expressed in knockout animal tissue by a 220 bp band (**Figure 9B**).

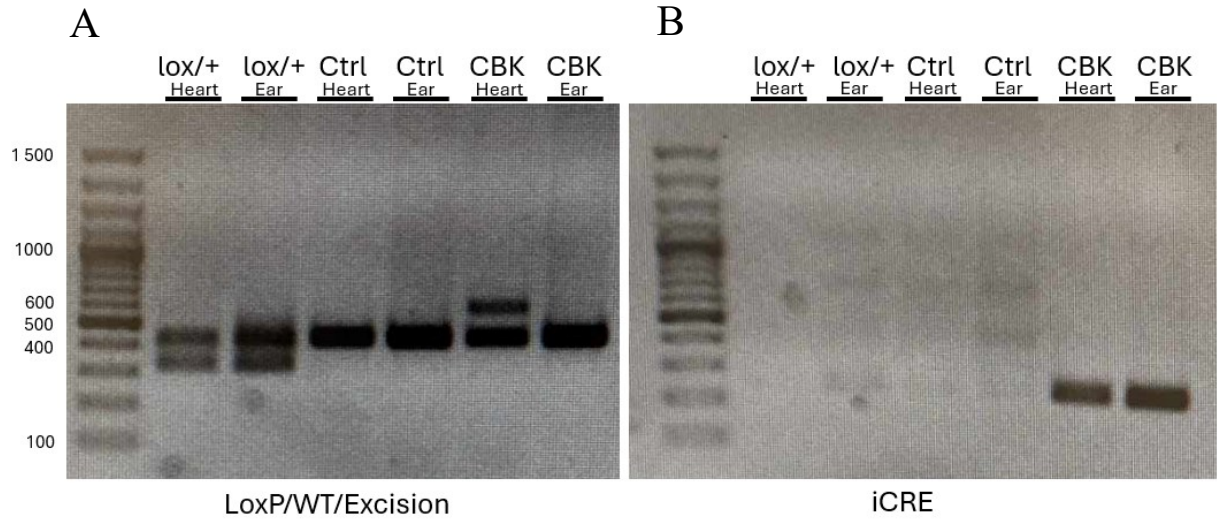

***Figure 9A**: Validation of Bmal1 knockout.*

***Figure 9B**: Cre expression in tissue.*

3.2 Validation of differences in BMAL1 protein expression using Immunoblotting

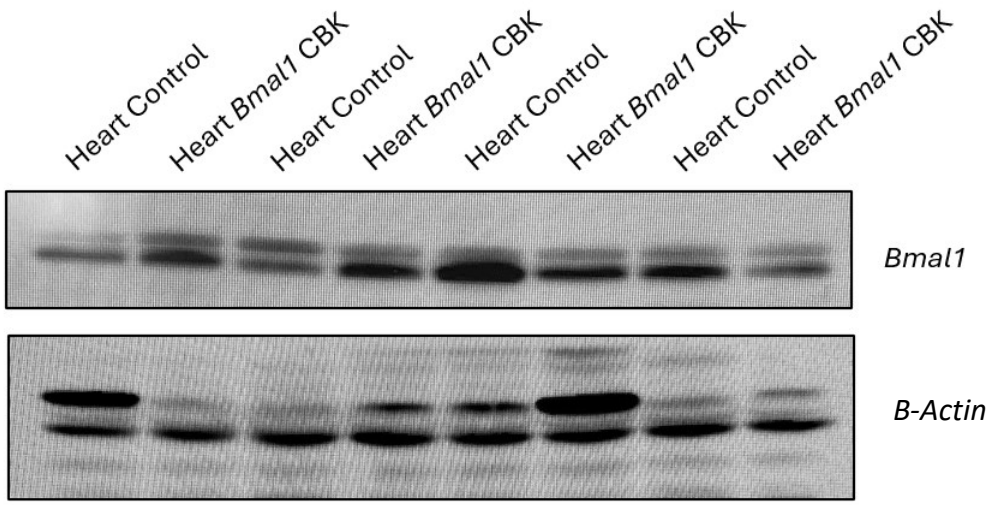

Figure 10: BMAL1 *protein expression was not different between control and experimental mice.*

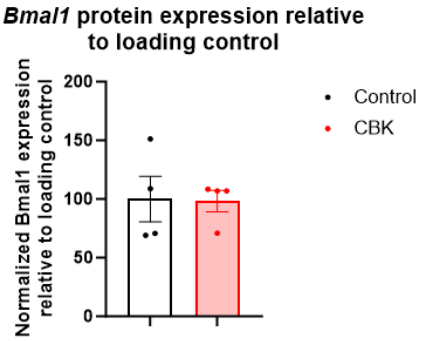

Figure 11: *Normalized* BMAL1 *protein expression relative to loading control.*

To validate the CBK model, we measured BMAL1 protein expression in heart tissue using Immunoblotting analysis. B-Actin was used as a loading control (**Figure 10**). We expected a significantly reduced expression of the BMAL1 protein band normalized to the expressed loading control band for CBK animals. **Figure 11** shows no significant differences in percent BMAL1

protein expression in heart tissue relative to controls between both groups (100 ± 38.78%; 98.3 ± 38.78 18.3%) (n = 4). Based on the outcomes, we conclude that the efficacy of the vector was insufficient at the used concentration to infect a significant number of cardiomyocytes to cause a chronic heart condition.

3.3 Cardiac phenotype assessment

A Two-way repeated measures ANOVA showed that the main effect of genotype was not statistically significant for the different cardiac phenotype variables ($p > 0.05$). Therefore, there were no differences between groups for all cardiac measures. We had hypothesized that heart function would degrade over time in CBK mice. Consequently, these results are in agreement with the failure to knockout *Bmal1* from a sufficient number of cardiomyocytes. Normality was confirmed using the Shapiro-Wilk normality test.

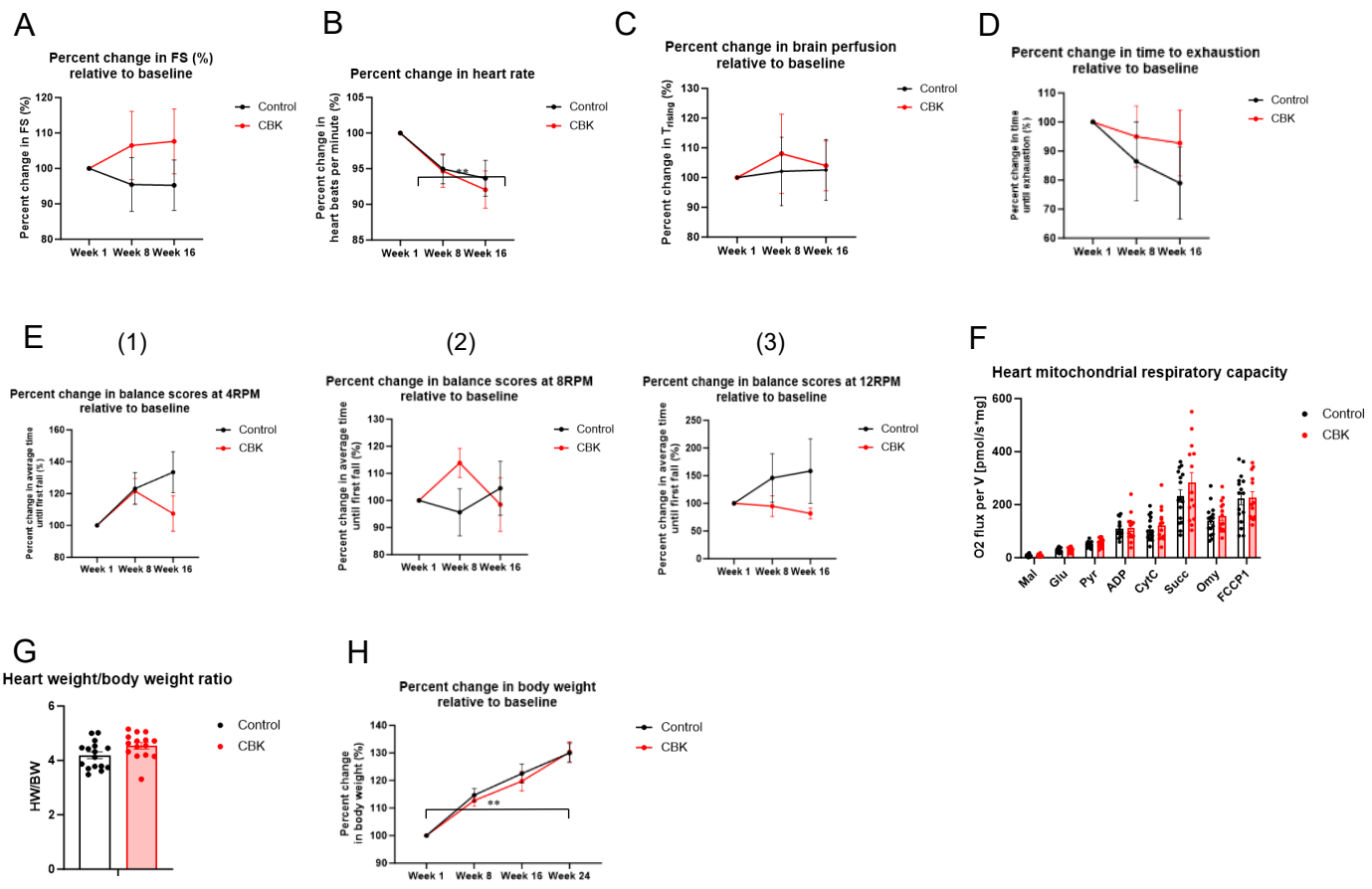

Figure 12. *Cardiac phenotypes data. (A) Change in fraction shortening measures relative to baseline taken from ultrasound image of LV M-mode of mice hearts. (B) Change in heart rate measured from ultrasound image of LV M-mode of mice hearts. (C) Change in time until fluorescent dye appears in brain relative to baseline during fluorescent imaging. (D) Change in time until exhaustion on treadmill test relative to baseline. (E) Change in balance scores over time relative to baseline at 4RPM (1), 8RPM (2) and 12 RPM (3). (F) Heart mitochondrial respiratory capacity for different substrates. (G) Heart weight/Body ratio as an indication of cardiac hypertrophy. (H) Change in body weight relative to baseline.*

3.3.1 Echocardiography

The change in fractional shortening (FS) (%) over time relative to baseline was not significantly different between control and CBK mice, suggesting that there were no differences in heart contractility between both groups ($p > 0.05$) (n = 12) (**Figure 12A**). Animals were excluded because of the inability to read ultrasound M-mode picture adequately. The average FS (%) across all weeks was calculated, where it was 36.79 ± 7.40% for controls and 33.30 ± 6.93% for CBK, both indications of no impaired cardiac contractility overall (Jia et al., 2018). Heart rate (bpm) was not significantly different between groups ($p > 0.05$) (n = 15) (**Figure 12B**). However, time did have a significant effect on heart rate ($p < .001$). A Tukey's multiple comparisons test revealed that heart rate was significantly different for both groups from week 1 to week 16 (**Table 2**) ($p < 0.05$).

	Week 1	Week 8	Week 16
Control	350 ± 77 bpm	317 ± 74 bpm	312 ± 73 bpm
CBK	349 ± 72 bpm	317 ± 72 bpm	310 ± 67 bpm

***Table 2**: Change in heart rate over time.*

3.3.2 Brain fluorescent imaging

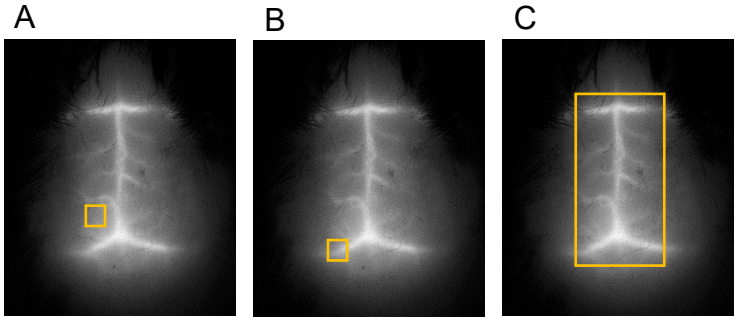

***Figure 13**: Area analysed to evaluate Trising (A) somatosensory cortical region. (B) Large vein (posterior left). (C) Large region.*

After the injection of indocyanine green, bolus dynamics captured by the infrared camera were analysed. Grey values of each pixel were measured in the *Fiji Software*. As a measure of brain perfusion, T_{rising} was calculated by subtracting $T_{arrival}$, the time of appearance dye at the brain, from the first peak time (T_{peak}). Dynamics of each pixel was evaluated for the somatosensory cortical region (**Figure 13A**), the region over the left posterior vein (**Figure 13B**) and a large region (**Figure 13C**). There was a significant difference between the T_{rising} times between all three regions. However, we evaluated that there was no significant difference between the average T_{rising} measures of the somatosensory cortical region and the posterior left suture, with that of the large area ($p > 0.05$). Therefore, we concluded that the large area T_{rising} values were representative of the status of overall tissue blood supply. This technique does not allow for specific quantification of blood flow to specific areas of the brain. Consequently, it served as a measure of general blood supply to cerebral tissue. Following injection of indocyanine green, brain perfusion measures from T_{rising} were similar between each group and over time, indication of no difference between groups and no longitudinal change in blood supply to the brain ($p > 0.05$) (n = 11 CBK; 10 Control) (**Figure 12C**). Animals were excluded because of a failure to properly inject the bolus for all timepoints. Considering there was no effect of time on brain perfusion, the average of all timepoints for each group was taken. Average T_{rising} was 1.67 ± 0.29s vs. 1.62 ± 0.31s for control and CBK animals respectively (Ku & Choi, 2012).

3.3.3 Treadmill

The main effect of genotype was not statistically significant ($p > 0.05$) (n = 15 CBK; 16 Control). Therefore, there were no significant differences in maximum aerobic capacity over time between CBK and control animals, shown by no change in the time until exhaustion on the

treadmill test between groups (**Figure 12D**). One animal did not make it through the study, so its data was excluded.

3.3.4 Rotarod

Genotype was not a source of variation in balance scores ($p > 0.05$) (n = 15 CBK; 16 Control). Therefore, there were no differences between both groups over time in balance scores relative to baseline at rotarod speeds of 4 RPM, 8 RPM and 12 RPM (**Figure 12E**).

3.3.5 Mitochondrial oxygen consumption

Both groups showed no difference in heart respiration rates, suggesting similar mitochondrial efficiency within heart tissue ($p > 0.05$) (n = 15 CBK; 16 Control) (**Figure 12F**).

3.3.6 Heart weight to body weight ratio

An unpaired T-Test showed no significant differences in heart weight to body weight ratios between control and CBK animals, revealing no induced cardiac hypertrophy over time ($p > 0.05$) (n = 15 CBK; 16 Control) (**Figure 12G**).

3.3.7 Body weight

Body weight for control and CBK mice was similar ($p > 0.05$). The change in weight over time relative to baseline for both groups was significantly different from week 1 to week 24 ($p < .001$) (n = 15 CBK; 16 Control) (**Figure 12H**).

3.4 Behavioral phenotype assessment

A Two-way repeated measures ANOVA revealed that the main effect of genotype was not statistically significant for all behavioral phenotypes assessments associated with depression ($p > 0.05$). We had hypothesized that cardiac impairments in CBK mice would cause increased expression of depressive-like behavior. Therefore, the lack of differences between each group may be because of the failure of the virus to remove *Bmal1* in a significant number of cardiomyocytes to cause an impaired heart function. Normality was confirmed using the Shapiro-Wilk normality test

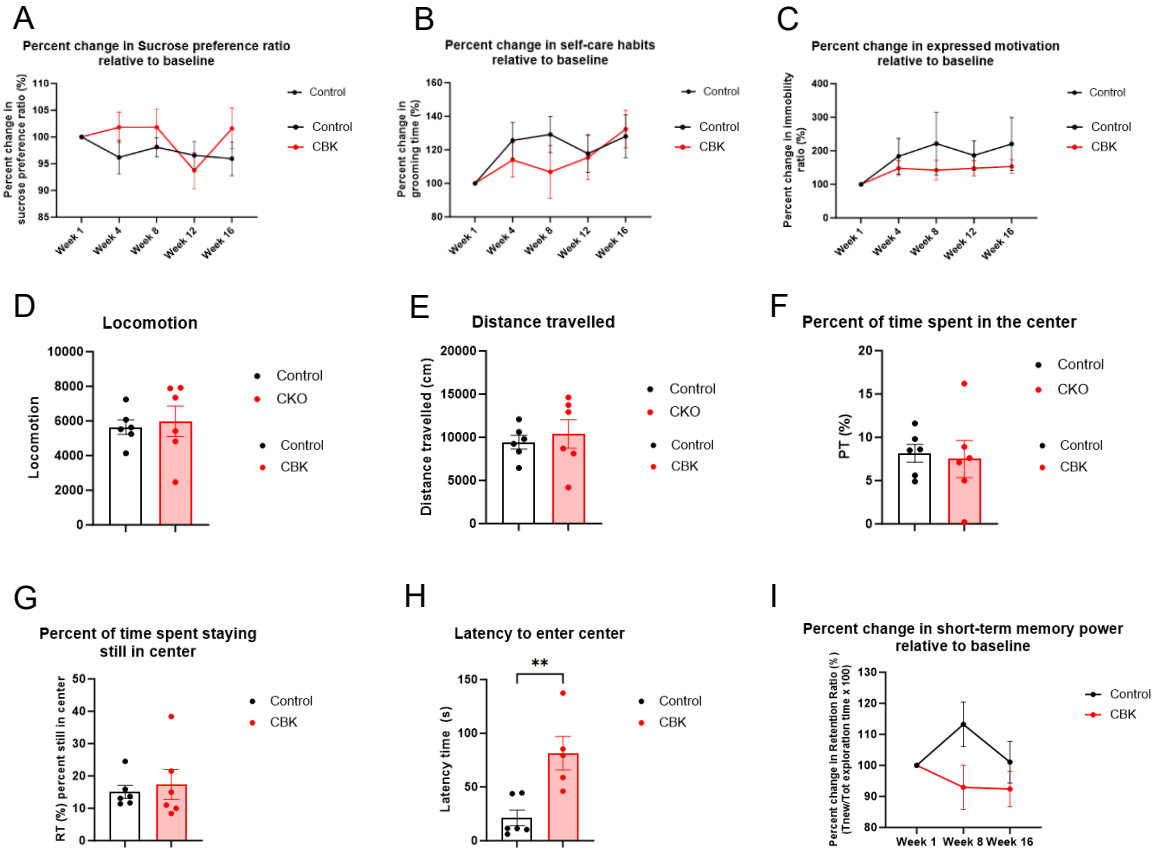

Figure 14. *Behavioral phenotypes data. (A) Change in sucrose preference over time as a measure of depressive-like anhedonia. (B) Change in grooming time in the splash test as a measure of self-care habits. (C) Change in immobility time in the tail suspension test to changes in expressed motivation. (D) Open field test (OFT) as a measure of anxiety-like behavior: locomotion. (E) OFT: Distance travelled. (F) OFT: Percent time spent in the center of the open field. (G). OFT: percent of time spent staying still in the centre of the open field. (H) OFT: Latency to enter the center of the open field. (I) Change in retention ratio in object recognition test as a measure of short-term memory.*

3.4.1 Sucrose preference test (SPT)

There was no difference in sucrose consumption between groups in the SPT, indicating similar levels of depression-like anhedonia ($p > 0.05$) (n = 13) (**Figure 14A**). Animals that had bottles leak were excluded from the analysis.

3.4.2 Splash test

There were no significant differences between change in grooming time relative to baseline between controls and CBK mice, suggesting similar levels of self-care habits over time for both groups ($p > 0.05$) (n = 12 CBK; 15 Control) (**Figure 14B**).

3.4.3 Tail suspension test

The immobility ratio (%) relative to baseline was not significantly different between control and experimental animals, suggesting no change in expressed motivation between groups over time ($p > 0.05$) (n = 7 CBK; 5 Control)) (**Figure 14C**). Animals were excluded because of a tail injury that prevented them from undergoing the test.

3.4.4 Open field test (OFT)

The Shapiro-Wilk test showed that the data was non-parametric ($p < 0.05$) (n = 6 CBK; 5 Control). A Mann-Whitney test revealed that controls did not spend significantly more time in the center, stand still in the center of the field and did not travel more distance compared to experimental animals ($p > 0.05$) (**Figure 14D-G**). However, CBK mice showed increased latency to enter the center of the field ($p = 0.005$) (**Figure 14H**). Animals were excluded because of lost data due to equipment failure.

3.4.5 Object recognition test

Genotype did not influence short-term memory over time, shown by similar retention ratios between CBK and control animals at each time point ($p > 0.05$) (n = 8) (**Figure 14I**). Animals with a total exploration time of less than 20sec were excluded from the analysis because recognition ratios were not reliable considering the small amount of time the animal spent with the objects.

4.0 Discussion

4.1 Validation of CBK model using PCR and Immunoblotting

The tests described above indicate a failure to knockout the *Bmal1* gene in cardiomyocytes of the experimental mice. Although the PCR testing confirmed that the AAV9-cTNT-Cre virus affected the heart through the expression of a knockout product specifically in heart tissue of the CBK mice, The concentration we used was insufficient to infect as many cells as needed to generate a heart condition. Considering that PCR utilizes the multiplication of the DNA sequence of interest, it is believed that only a small proportion of genes were affected by the viral vectors, consequently preventing effective elimination of *Bmal1* in cardiomyocytes to induce a heart dysfunction. The knockout product was detected by PCR solely because it was replicated multiple times during the thermocycling process. Since genes serve to specify amino acid sequences and proteins are responsible for all cellular function, protein expression is a more accurate measure of the CBK model's efficacy (Koussounadis et al., 2015). Consequently, according to the protein expression analysis, the virus failed to remove *Bmal1* in a significant number of cardiomyocytes to cause an impaired heart function.

4.2 Reasons for the lack of virus efficiency

4.2.1 Virus viability

AAV9 vectors are non-enveloped viruses made up of single stands of DNA and contained in capsids. Despite advancements in manufacturing to improve viral stability and infectibility, several factors may contribute to its degradation. Firstly, viral particle can be lost due to contact with surfaces or during freezing. Viral core facilities have developed formulas that use a

cryoprotectant or a substance to guard against degradation when in contact with surfaces, but excessive manipulation and repeated freeze-thaw cycles at -80C remain significant risks for viral genome particles loss (Chan et al., 2022). Therefore, potential freeze-thaw cycles in transit from the supplier in Germany could have contributed to virus degradation. Additionally, from the time we diluted the virus until the administration with the intravenous injection, many particles could have been destroyed due to contact with surfaces such as tests tubes and syringes. The loss of genome particles could have reduced the concentration of the virus to a level that was insufficient to cause a significant knockout of *Bmal1* in cardiomyocytes.

4.2.2 Dosage

The AAV9-cTNT-Cre injected was $1x10^{11}$ viral genomes ($1x10^{13}$ vg/mL, 100uL) Typically, AAV vectors are purified viral particles in phosphate buffered saline at a concentration of $1x10^{12}$ particles/mL (Safety & Handling | UNC Vector Core, n.d.). Despite injecting an amount that is on the lower end of these recommendations, there still should have been a significant knockout of *Bmal1* in cardiomyocytes. Consequently, virus viability could have drastically affected the viral vector concentrations, contributing to the inability to modify a significant number of cells to cause heart dysfunction. Future studies using this type of viral vectors should test stronger concentrations of particle/mL to verify if the dosage used was the issue in this study.

4.2.1 Viral Antibodies

The administration of adeno-associated virus serotype 9 (AAV9) is a technique used to deliver specific genes using AAV inverted terminal repeats flanking the target DNA sequence (*Flanking Sequence - Terminology of Molecular Biology for Flanking Sequence – GenScript*, 2024). AAV is the preferred vector for in vivo gene transfer because of its safety, versatility in targeting several tissues, and ability to carry many viral genomes with distinct effects. However, the use of viral vectors can be complicated by the potential of immune responses, which is a substantial challenge with their use (Shirley et al., 2020). Studies have shown that AAV9 neutralizing antibodies exist, as demonstrated in Chinese patients with Duchenne muscular dystrophy (C. Wei et al., 2024). This observation in humans may suggest that antibodies against the AAV9-cTNT virus could also neutralize its effects in mice following intravenous administration.

In this study, the viral vectors used was specific to gene sequence Cardiac troponin T (cTNT), a cardiac isoform used as a marker of myocardial cell injury. The virus was manufactured to use Cre recombinase to selectively remove *Bmal1* from cardiomyocytes through the AAV delivery to cTNT. While this cardiac specific promoter increases specificity, the degree of expression from tissue-restricted promoters may not be as high as global viral promoters (Ambrosi et al., 2019). Consequently, even a minor immune response could significantly reduce the virus' efficacy due to lower expression levels.

4.3 Cardiac phenotypes prove lack of virus efficiency

The knockout of *Bmal1* was expected to cause cardiac abnormalities progressively, where we would have seen significant decreases in heart contractility, heart rate, brain perfusion measures, cardiovascular endurance, balance, and mitochondrial efficiency in CBK mice compared to controls. However, the cardiac phenotypes assessments shown above demonstrate no significant differences over time between control and CBK groups, in agreement with the failure of the virus to delete *Bmal1* in a significant number of cardiomyocytes to cause heart dysfunction.

4.3.1 Ultrasound measurement

Normal fractional shortening (FS) (%) in adult mice anesthetized with isoflurane is 39 ± 1%, with decreases in FS(%) indicating cardiac dysfunction due to decreases in contractile force during systole (Gao et al., 2011; Murphy et al., 2022). For example, FS (%) measured in mice 3 weeks following transverse aortic constriction was below 25% (Gao et al., 2011). This current study found no significant difference in FS (%) over time between the groups, indicating no change in heart contractility (**Figure 13A**). If the virus had been effective, a lower FS (%) in the experimental group compared to controls would have been expected because of heart dysfunction caused by the removal of *Bmal1* in heart muscle cells.

To follow, changes in heart rate were measured over time from the same ultrasound M-mode images. Although the number of beats per minute was not different between groups, there was a significant decrease over time (**Figure 13B**). This reduction in heart rate can be attributed to age-related changes or to the time under anesthesia. Heart rate naturally decreases with age in B57 mice, so a small percentage of the change may have been related to aging (Xing et al., 2009).

The mice began the study at 8 weeks old and completed the final tests at 33 weeks old (7.5 months), classifying them as mature adults to just approaching middle age (10 months).

The duration under anesthesia depended on the ease of capturing the ultrasound image, potentially influencing the cardiac parameters. Longer times under the influence of isoflurane (2%) could have decreased heart rate for some animals, as data acquisition was more challenging for some weeks (Roth et al., 2002). Unfortunately, the duration of anesthesia was not logged, which should be addressed in the future studies.

4.3.2 Brain fluorescent imaging

This technique measured general cerebral perfusion by analyzing bolus dynamics following an intravenous injection of indocyanine green. In cases of heart failure, we expected cerebral perfusion to decreased due to impaired cardiac function. Consequently, a successful knockout of *Bmal1* in cardiomyocytes was anticipated to result in higher T_{rising} times in the experimental group compared to controls. Decreased heart contractility from cardiac remodeling would lead to larger times for the bolus to reach the brain because of reduced pressures. However, consistent with the failure to induce heart dysfunction, brain perfusion measures from T_{rising} were similar between each group over time, indication of no change in blood supply to the brain (**Figure 13C**).

4.3.3 Treadmill

Maximum aerobic endurance was used as a measure of cardiac health. The time until exhaustion was expected to decrease more substantially in CBK mice compared to controls because of the heart condition limiting the supply of oxygenated blood to the periphery. However,

in line with the lack of induced heart failure, no significant differences in maximum aerobic capacity were observed over time between CBK and control animals. This was demonstrated by similar times until exhaustion on the treadmill test across both groups (**Figure 14D**).

4.3.4 Rotarod

The rotarod test, which assesses balance and coordination, was chosen to determine if reduced peripheral perfusion caused by heart failure would lead to any motor deficits. We hypothesized that such deficits would arise from morphological changes in the cerebellum secondary to poor brain perfusion in heart failure (Surgent et al., 2019). Considering the absence of heart impairment, genotype did not contribute to variation in balance scores between both groups over time at rotarod speeds of 4 RPM, 8 RPM and 12 RPM (**Figure 13E**). Therefore, the systems regulating balance and coordination remained unaffected in both groups.

4.3.5 Mitochondrial oxygen consumption

Mitochondria occupy a large portion of the adult heart, where their ability to metabolize oxygen and convert it into energy is essential for proper cardiac function. One mechanism of heart failure is inadequate energy supply from dysfunctional mitochondria (Tian et al., 2019). Therefore, we expected that the deletion of the *Bmal1* clock gene would result in lower mitochondrial respiratory capacity in experimental animals compared to controls. However, because of the inability to induce heart failure, mice from both groups showed no differences in heart respiration rates, suggesting similar mitochondrial efficiency within the heart tissue.

4.3.6 Heart weight to body weight ratio

This ratio measured levels of hypertrophy in response to the absence of *Bmal1* in cardiomyocytes. Larger values would suggest increased heart dysfunction, with a healthy ratio being around 3.86 ± 0.18 (Jia et al., 2018). Values obtained were healthy (**Figure 13G**). There was no difference in heart weight to body weight ratios between control and CBK animals, revealing no induced cardiac hypertrophy over time. As body weight increased in both groups, this was accompanied with larger heart weights to account for large cardiac outputs in these animals (Jia et al., 2018). Therefore, ratios would remain unchanged unless cardiac hypertrophy was present.

4.3.7 Body weight

Body weight was not significantly different between control and CBK mice. We hypothesized that mice with heart failure would have larger body weights because of increased sedentary behavior resulting from lower fitness levels associated with heart disease. Both groups showed a significant increase in weight over time relative to baseline from week 1 to week 24. This weight gain could be attributed to aging, unlimited food supply and sedentary behavior in cages.

4.4 Behavioral phenotypes prove lack of virus efficiency

The knockout of *Bmal1* was expected to cause behavior abnormalities, characterized by significant expression of depressive-like phenotypes such as decreased desire for pleasurable things, motivation and self-care. Additionally, we expected increases in anxiety-related behavior in CBK compared to controls. However, the phenotypes assessments shown above demonstrated

no significant differences over time between control and CBK groups. These results could potentially be attributed to the inability to induce heart failure in the experimental group.

4.4.1 Sucrose preference test

This test assessed levels of anhedonia, a strong endophenotype of depression. The regulation of positive emotions typically involved the identification of a stimulus to produce an affective state (Gorwood, 2008). Identification occurs in the ventral regions like the amygdala, insula, ventral striatum, and ventral regions of the anterior cingulate gyrus and prefrontal cortex. Additionally, the dorsal system is involved in executing a function according to the positive emotions (Gorwood, 2008). Consequently, heart dysfunction was expected to cause alterations in these brain areas regulating mood and cause a decrease in sucrose consumption over time in the CBK group. However, no differences in sucrose consumption were observed between groups, indicating that the expression of this emotional phenotype remained unaltered over time.

4.4.2 Splash test

Grooming time was anticipated to decrease for experimental animals. Considering that a reduction in self-care habits is an important phenotype of depression, we expected regions like the basal ganglia, which is responsible for habit development, to be affected by the heart dysfunction (Smith & Graybiel, 2016). However, this study revealed no significant differences in the change in grooming time relative to baseline between controls and CBK mice, suggesting similar levels of self-care habits over time for both groups. The absence of cardiac impairment may have prevented morphological changes in brain regions regulating self-care habits.

4.4.3 Tail suspension test

Reduced motivation is a key component of depression, where inner will power was measured from the time spent immobile while suspended by the tail. Immobility time was hypthesized to increase over time because of brain alterations secondary to heart failure, which could include downregulation of the activity in the ventral striatum that controls emotions like motivation. However, consistent with the inability to knockout *Bmal1* in cardiomyocytes, the immobility ratio (%) relative to baseline was not significantly different between control and experimental animals, suggesting no differences in expressed motivation between groups over time. This indicates that brain regions that control this emotion were not affected.

4.4.4 Open field test (OFT)

Anxiety is believed to originate from the activation of the right anterior insula and adjacent regions in response to the prediction of negative events (Sasaoka et al., 2022). This emotion was evaluated with the OFT because it often accompanies depression, serving as another endophenotype that could provide insights about the animal's state of mind. In this study, controls did not spend significantly more time in the center, stand still in the center of the field and did not travel more distance compared to experimental animals, thus indicating no differences in expressed anxiety-like behavior related to exploration. However, the injection of *Bmal1* cardiomyocyte knockout viral vectors did influence the latency to enter the center of the field, suggesting differences in anxiety-related exploration of new spaces. Future studies would be needed to explain these differences considering that in this case, *Bmal1* knockout in cardiomyocytes was not sufficient to induce a chronic heart condition.

4.4.5 Object recognition test

Short-term memory was expected to decrease more significantly in CBK mice compared to control mice. Heart abnormalities were expected to cause alteration in the hypothalamus from reduced blood supply, the brain region responsible short-term memory regulation. The test was chosen because individuals diagnosed with depression demonstrate increased cases of impaired memory recollection compared to healthy adults (Dillon & Pizzagalli, 2018). Given that this study aimed to test for a depressive-like phenotype based on the hypothesis that reduced blood flow to the brain was causing morphological and physiological changes leading to mood alterations, a memory consolidation evaluation was included to provide further insights on the mice's mental state. This study found that genotype did not influence short-term memory over time, shown by similar retention ratios between CBK and control animals at each time point. The failure of the virus to delete *Bmal1* in a significant number of cardiomyocytes to cause heart dysfunction could explain the lack of differences between the groups.

5.0 Conclusion

This would have been the first study to look at how cardiac phenotypes change following progressively induced heart failure and relate the severity of heart dysfunction to alterations in behavior. Although PCR analysis confirmed *Bmal1* knockout at the gene expression level, the evaluation of protein expression failed to identify successful removal of this clock gene in cardiomyocytes. As a result, no cardiac impairments developed over time. Several factors could have contributed to this outcome, including incorrect dosage administration, issues with the viability of the viral vectors or an immune response to the injection bolus. The inability to cause heart failure with the AAV9-cTNT-Cre injection was consistent with the results of the study, which

demonstrated no significant differences in cardiac function between groups. Consequently, this may explain why behavioral phenotypes between control and experimental animals were also similar.

This study could have provided individuals with cardiovascular disease a timeline of depression risk and potential reasons why their mental health is degrading following their diagnosis. Providing additional foundational knowledge about the heart-brain relationship is still necessary to improve the prognosis for individuals diagnosed with heart failure and depression. Therefore, there is still large value in future research on this topic to better patient outcomes.

When this study is redone, the effects of the administration of a stronger dose concentration of the viral vectors on protein expression of BMAL1 would need to be evaluated. Longitudinally, change in cardiac phenotypes would need to be investigated to confirm that the *Bmal1* knockout in cardiomyocytes has the desired effects on heart tissue.

5.1 Future considerations

If I were to redo this study, I would start by performing a protein expression analysis of BMAL1 expression in CBK mice at the beginning of the experiment. This verification step would have confirmed the inefficiency of the viral vector. Considering that the viability was a potential reason for the ineffective viral vector, future experiments should test the efficiency of *Bmal1* deletion by using larger concentrations of the virus and measuring differences in BMAL1 protein expression in heart tissue. If higher concentrations prove effective in deleting *Bmal1* in cardiomyocytes, the next step would be to verify if cardiovascular impairments develop and correlate these changes with mood alterations over time.

6.0 References

Ambrosi, C. M., Sadananda, G., Han, J. L., & Entcheva, E. (2019). Adeno-Associated Virus Mediated Gene Delivery: Implications for Scalable in vitro and in vivo Cardiac Optogenetic Models. *Frontiers in Physiology*, *10*. https://doi.org/10.3389/fphys.2019.00168

Azevedo, P. S., Polegato, B. F., Minicucci, M. F., Paiva, S. A. R., & Zornoff, L. A. M. (2016). Cardiac Remodeling: Concepts, Clinical Impact, Pathophysiological Mechanisms and Pharmacologic Treatment. *Arquivos Brasileiros de Cardiologia*. https://doi.org/10.5935/abc.20160005

Belovicova, K., Bogi, E., Csatlosova, K., & Dubovicky, M. (2017). Animal tests for anxiety-like and depression-like behavior in rats. *Interdisciplinary Toxicology*, *10*(1), 40–43. https://doi.org/10.1515/intox-2017-0006

Bouguiyoud, N., Roullet, F., Bronchti, G., Frasnelli, J., & Al Aïn, S. (2022). Anxiety and Depression Assessments in a Mouse Model of Congenital Blindness. *Frontiers in Neuroscience*, *15*, 807434. https://doi.org/10.3389/fnins.2021.807434

Boyette, L. C., & Manna, B. (n.d.). Physiology, Myocardial Oxygen Demand. *StatPearls*. https://www.ncbi.nlm.nih.gov/books/NBK499897/

Bruss, Z. S., & Raja, A. (2024). Physiology, Stroke Volume. In *StatPearls*. StatPearls Publishing. http://www.ncbi.nlm.nih.gov/books/NBK547686/

Can, A., Dao, D. T., Terrillion, C. E., Piantadosi, S. C., Bhat, S., & Gould, T. D. (2011). The Tail Suspension Test. *Journal of Visualized Experiments*, *58*, 3769. https://doi.org/10.3791/3769

Celano, C. M., & Huffman, J. C. (2018). Heart Failure and Suicide: The Role of Depression. *Journal of Cardiac Failure*, *24*(11), 801–802. https://doi.org/10.1016/j.cardfail.2018.10.003

Chan, A., Maturana, C. J., & Engel, E. A. (2022). Optimized formulation buffer preserves adeno-associated virus-9 infectivity after 4 °C storage and freeze/thawing cycling. *Journal of Virological Methods*, *309*, 114598. https://doi.org/10.1016/j.jviromet.2022.114598

Chu, B., Marwaha, K., Sanvictores, T., & Ayers, D. (2024). Physiology, Stress Reaction. In *StatPearls*. StatPearls Publishing. http://www.ncbi.nlm.nih.gov/books/NBK541120/

Crnko, S., C, D. P. B., Sluijter, J. P., & W, V. L. L. (2019). Circadian rhythms and the molecular clock in cardiovascular biology and disease. *Nature Reviews. Cardiology*, *16*(7), 437–447. https://doi.org/10.1038/s41569-019-0167-4

Cryan, J. F., Mombereau, C., & Vassout, A. (2005). The tail suspension test as a model for assessing antidepressant activity: Review of pharmacological and genetic studies in mice. *Neuroscience & Biobehavioral Reviews*, *29*(4–5), 571–625. https://doi.org/10.1016/j.neubiorev.2005.03.009

Curtis, A. M., Cheng, Y., Kapoor, S., Reilly, D., Price, T. S., & FitzGerald, G. A. (2007). Circadian variation of blood pressure and the vascular response to asynchronous stress.

Proceedings of the National Academy of Sciences, *104*(9), 3450–3455. https://doi.org/10.1073/pnas.0611680104

d'Isa, R., & Gerlai, R. (2023). Designing animal-friendly behavioral tests for neuroscience research: The importance of an ethological approach. *Frontiers in Behavioral Neuroscience*, *16*, 1090248. https://doi.org/10.3389/fnbeh.2022.1090248

Davidson, A. J., London, B., Block, G. D., & Menaker, M. (n.d.). *Cardiovascular Tissues Contain Independent Circadian Clocks*.

Delong, C., & Sharma, S. (2023). Physiology, Peripheral Vascular Resistance. *StatPearls*. https://www.ncbi.nlm.nih.gov/books/NBK538308/

DiGiuseppe, R., David, D., & Venezia, R. (2016). Cognitive theories. In J. C. Norcross, G. R. VandenBos, D. K. Freedheim, & B. O. Olatunji (Eds.), *APA handbook of clinical psychology: Theory and research (Vol. 2).* (pp. 145–182). American Psychological Association. https://doi.org/10.1037/14773-006

Dillon, D. G., & Pizzagalli, D. A. (2018). Mechanisms of Memory Disruption in Depression. *Trends in Neurosciences*, *41*(3), 137–149. https://doi.org/10.1016/j.tins.2017.12.006

flanking sequence—Terminology of Molecular Biology for flanking sequence – GenScript. (n.d.). Retrieved April 11, 2024, from https://www.genscript.com/biology-glossary/1096/flanking-sequence

French, B. A., & Annex, B. H. (2014). AAV9 and Cre: A one-two punch for a quick cardiac knockout. *Cardiovascular Research*, *104*(1), 3–4. https://doi.org/10.1093/cvr/cvu200

Frey, A., Popp, S., Post, A., Langer, S., Lehmann, M., Hofmann, U., SirÃ©n, A.-L., Hommers, L., Schmitt, A., Strekalova, T., Ertl, G., Lesch, K.-P., & Frantz, S. (2014). Experimental heart failure causes depression-like behavior together with differential regulation of inflammatory and structural genes in the brain. *Frontiers in Behavioral Neuroscience*, *8*. https://doi.org/10.3389/fnbeh.2014.00376

Gao, S., Ho, D., Vatner, D. E., & Vatner, S. F. (2011). Echocardiography in Mice. *Current Protocols in Mouse Biology*, *1*(1), 71–83. https://doi.org/10.1002/9780470942390.mo100130

Garibyan, L., & Avashia, N. (2013). Research Techniques Made Simple: Polymerase Chain Reaction (PCR). *The Journal of Investigative Dermatology*, *133*(3), e6. https://doi.org/10.1038/jid.2013.1

Ge, Z., Li, A., McNamara, J., Dos Remedios, C., & Lal, S. (2019). Pathogenesis and pathophysiology of heart failure with reduced ejection fraction: Translation to human studies. *Heart Failure Reviews*, *24*(5), 743–758. https://doi.org/10.1007/s10741-019-09806-0

Gilbert, G., Demydenko, K., Dries, E., Puertas, R. D., Jin, X., Sipido, K., & Roderick, H. L. (2020). Calcium Signaling in Cardiomyocyte Function. *Cold Spring Harbor Perspectives in Biology*, *12*(3), a035428. https://doi.org/10.1101/cshperspect.a035428

Gordan, R., Gwathmey, J. K., & Xie, L.-H. (2015). Autonomic and endocrine control of cardiovascular function. *World Journal of Cardiology*, *7*(4), 204. https://doi.org/10.4330/wjc.v7.i4.204

Gorwood, P. (2008). Neurobiological mechanisms of anhedonia. *Dialogues in Clinical Neuroscience*, *10*(3), 291–299.

Gould, T. D., Dao, D. T., & Kovacsics, C. E. (2009). The Open Field Test. In T. D. Gould (Ed.), *Mood and Anxiety Related Phenotypes in Mice: Characterization Using Behavioral Tests* (pp. 1–20). Humana Press. https://doi.org/10.1007/978-1-60761-303-9_1

Hånell, A., & Marklund, N. (2014). Structured evaluation of rodent behavioral tests used in drug discovery research. *Frontiers in Behavioral Neuroscience*, *8*. https://doi.org/10.3389/fnbeh.2014.00252

Harrison, F. E., Hosseini, A. H., & McDonald, M. P. (2009). Endogenous anxiety and stress responses in water maze and Barnes maze spatial memory tasks. *Behavioural Brain Research*, *198*(1), 247–251. https://doi.org/10.1016/j.bbr.2008.10.015

Hazar-Yavuz, A. N., Keles, R., Unal, G., Taskin, T., & Aricioglu, F. (n.d.). *ANTIDEPRESSANT LIKE EFFECT OF HYDRO-ALCOHOLIC EXTRACT OF NIGELLA SATIVA IN TAIL SUSPENSION TEST IN MICE*.

Hong, T., & Shaw, R. M. (2017). Cardiac T-Tubule Microanatomy and Function. *Physiological Reviews*, *97*(1), 227–252. https://doi.org/10.1152/physrev.00037.2015

Iliesiu, A., Campeanu, A., Marta, D., Parvu, I., & Gheorghe, G. (2015). Uric Acid, Oxidative Stress and Inflammation in Chronic Heart Failure with Reduced Ejection Fraction. *Revista Romana de Medicina de Laborator*, *23*(4), 397–406. https://doi.org/10.1515/rrlm-2015-0039

Jia, Z., Chen, Z., Xu, H., Armah, M. A., Teng, P., Li, W., Jian, D., Ma, L., & Ni, Y. (2018). Pressure Overload-induced Cardiac Hypertrophy Varies According to Different Ligation Needle Sizes and Body Weights in Mice. *Arquivos Brasileiros de Cardiologia*, *110*(6), 568–576. https://doi.org/10.5935/abc.20180088

Katz, R. J. (1982). Animal model of depression: Pharmacological sensitivity of a hedonic deficit. *Pharmacology, Biochemistry, and Behavior*, *16*(6), 965–968. https://doi.org/10.1016/0091-3057(82)90053-3

Kim, H., Kim, M., Im, S.-K., & Fang, S. (2018). Mouse Cre-LoxP system: General principles to determine tissue-specific roles of target genes. *Laboratory Animal Research*, *34*(4), 147–159. https://doi.org/10.5625/lar.2018.34.4.147

King, J., & Lowery, D. R. (2024). Physiology, Cardiac Output. In *StatPearls*. StatPearls Publishing. http://www.ncbi.nlm.nih.gov/books/NBK470455/

Kondratov, R. V., Kondratova, A. A., Gorbacheva, V. Y., Vykhovanets, O. V., & Antoch, M. P. (2006). Early aging and age-related pathologies in mice deficient in BMAL1, the core componentof the circadian clock. *Genes & Development*, *20*(14), 1868–1873. https://doi.org/10.1101/gad.1432206

Koussounadis, A., Langdon, S. P., Um, I. H., Harrison, D. J., & Smith, V. A. (2015). Relationship between differentially expressed mRNA and mRNA-protein correlations in a xenograft model system. *Scientific Reports*, *5*(1), 10775. https://doi.org/10.1038/srep10775

Ku, T., & Choi, C. (2012). Noninvasive Optical Measurement of Cerebral Blood Flow in Mice Using Molecular Dynamics Analysis of Indocyanine Green. *PLoS ONE*, *7*(10), e48383. https://doi.org/10.1371/journal.pone.0048383

Kuznetsov, A. V., Veksler, V., Gellerich, F. N., Saks, V., Margreiter, R., & Kunz, W. S. (2008). Analysis of mitochondrial function in situ in permeabilized muscle fibers, tissues and cells. *Nature Protocols*, *3*(6), 965–976. https://doi.org/10.1038/nprot.2008.61

La Rovere, M. T., & Christensen, J. H. (2015). The autonomic nervous system and cardiovascular disease: Role of n-3 PUFAs. *Vascular Pharmacology*, *71*, 1–10. https://doi.org/10.1016/j.vph.2015.02.005

Ledoux, J., Gee, D. M., & Leblanc, N. (2003). Increased peripheral resistance in heart failure: New evidence suggests an alteration in vascular smooth muscle function. *British Journal of Pharmacology*, *139*(7), 1245–1248. https://doi.org/10.1038/sj.bjp.0705366

Li, E., Li, X., Huang, J., Xu, C., Liang, Q., Ren, K., Bai, A., Lu, C., Qian, R., & Sun, N. (2020). BMAL1 regulates mitochondrial fission and mitophagy through mitochondrial protein BNIP3 and is critical in the development of dilated cardiomyopathy. *Protein & Cell*, *11*(9), 661–679. https://doi.org/10.1007/s13238-020-00713-x

Lymperopoulos, A., Rengo, G., & Koch, W. J. (2013). Adrenergic Nervous System in Heart Failure: Pathophysiology and Therapy. *Circulation Research*, *113*(6), 739–753. https://doi.org/10.1161/CIRCRESAHA.113.300308

Malik, A., Brito, D., Vaqar, S., & Chhabra, L. (2024). Congestive Heart Failure. In *StatPearls*. StatPearls Publishing. http://www.ncbi.nlm.nih.gov/books/NBK430873/

Mao, Y., Xu, Y., & Yuan, X. (2022). Validity of chronic restraint stress for modeling anhedonic-like behavior in rodents: A systematic review and meta-analysis. *The Journal of International Medical Research*, *50*(2), 3000605221075816. https://doi.org/10.1177/03000605221075816

Mihl, C., Dassen, W. R. M., & Kuipers, H. (2008). Cardiac remodelling: Concentric versus eccentric hypertrophy in strength and endurance athletes. *Netherlands Heart Journal*, *16*(4), 129–133. https://doi.org/10.1007/BF03086131

Murphy, J., Le, T. N. V., Fedorova, J., Yang, Y., Krause-Hauch, M., Davitt, K., Zoungrana, L. I., Fatmi, M. K., Lesnefsky, E. J., Li, J., & Ren, D. (2022). The Cardiac Dysfunction Caused by Metabolic Alterations in Alzheimer's Disease. *Frontiers in Cardiovascular Medicine*, *9*, 850538. https://doi.org/10.3389/fcvm.2022.850538

Naso, M. F., Tomkowicz, B., Perry, W. L., & Strohl, W. R. (2017). Adeno-Associated Virus (AAV) as a Vector for Gene Therapy. *Biodrugs*, *31*(4), 317–334. https://doi.org/10.1007/s40259-017-0234-5

Olbert, C. M., Gala, G. J., & Tupler, L. A. (2014). Quantifying heterogeneity attributable to polythetic diagnostic criteria: Theoretical framework and empirical application. *Journal of Abnormal Psychology*, *123*(2), 452–462. https://doi.org/10.1037/a0036068

Planchez, B., Surget, A., & Belzung, C. (2019). Animal models of major depression: Drawbacks and challenges. *Journal of Neural Transmission*, *126*(11), 1383–1408. https://doi.org/10.1007/s00702-019-02084-y

Regitz-Zagrosek, V. (2020). Sex and Gender Differences in Heart Failure. *International Journal of Heart Failure*, *2*(3), 157. https://doi.org/10.36628/ijhf.2020.0004

Roth, D. M., Swaney, J. S., Dalton, N. D., Gilpin, E. A., & Ross, J. (2002). Impact of anesthesia on cardiac function during echocardiography in mice. *American Journal of Physiology-Heart and Circulatory Physiology*, *282*(6), H2134–H2140. https://doi.org/10.1152/ajpheart.00845.2001

Rustad, J. K., Stern, T. A., Hebert, K. A., & Musselman, D. L. (2013). Diagnosis and Treatment of Depression in Patients With Congestive Heart Failure: A Review of the Literature. *The Primary Care Companion for CNS Disorders*, *15*(4), PCC.13r01511. https://doi.org/10.4088/PCC.13r01511

Safety & Handling | UNC Vector Core. (n.d.). Retrieved April 11, 2024, from https://www.med.unc.edu/genetherapy/vectorcore/safety-handling/

Sasaoka, T., Harada, T., Sato, D., Michida, N., Yonezawa, H., Takayama, M., Nouzawa, T., & Yamawaki, S. (2022). Neural basis for anxiety and anxiety-related physiological responses during a driving situation: An fMRI study. *Cerebral Cortex Communications*, *3*(3), tgac025. https://doi.org/10.1093/texcom/tgac025

Savarese, G., Becher, P. M., Lund, L. H., Seferovic, P., Rosano, G. M. C., & Coats, A. J. S. (2023). Global burden of heart failure: A comprehensive and updated review of epidemiology. *Cardiovascular Research*, *118*(17), 3272–3287. https://doi.org/10.1093/cvr/cvac013

Sbolli, M., Fiuzat, M., Cani, D., & O'Connor, C. M. (2020). Depression and heart failure: The lonely comorbidity. *European Journal of Heart Failure*, *22*(11), 2007–2017. https://doi.org/10.1002/ejhf.1865

Schwinger, R. H. G. (2021). Pathophysiology of heart failure. *Cardiovascular Diagnosis and Therapy*, *11*(1), 263–276. https://doi.org/10.21037/cdt-20-302

Segelcke, D., Talbot, S. R., Palme, R., La Porta, C., Pogatzki-Zahn, E., Bleich, A., & Tappe-Theodor, A. (2023). Experimenter familiarization is a crucial prerequisite for assessing behavioral outcomes and reduces stress in mice not only under chronic pain conditions. *Scientific Reports*, *13*(1), 2289. https://doi.org/10.1038/s41598-023-29052-7

Seibenhener, M. L., & Wooten, M. C. (2015). Use of the Open Field Maze to Measure Locomotor and Anxiety-like Behavior in Mice. *Journal of Visualized Experiments*, *96*, 52434. https://doi.org/10.3791/52434

Shirley, J. L., De Jong, Y. P., Terhorst, C., & Herzog, R. W. (2020). Immune Responses to Viral Gene Therapy Vectors. *Molecular Therapy*, *28*(3), 709–722. https://doi.org/10.1016/j.ymthe.2020.01.001

Smith, K. S., & Graybiel, A. M. (2016). Habit formation. *Dialogues in Clinical Neuroscience*, *18*(1), 33–43.

Steru, L., Chermat, R., Thierry, B., & Simon, P. (1985). The tail suspension test: A new method for screening antidepressants in mice. *Psychopharmacology*, *85*, 367–370. https://doi.org/10.1007/BF00428203

Stukalin, Y., Lan, A., & Einat, H. (2020). Revisiting the validity of the mouse tail suspension test: Systematic review and meta-analysis of the effects of prototypic antidepressants. *Neuroscience and Biobehavioral Reviews*, *112*, 39–47. https://doi.org/10.1016/j.neubiorev.2020.01.034

Surgent, O. J., Dadalko, O. I., Pickett, K. A., & Travers, B. G. (2019). Balance and the Brain: A Review of Structural Brain Correlates of Postural Balance and Balance Training in Humans. *Gait & Posture*, *71*, 245–252. https://doi.org/10.1016/j.gaitpost.2019.05.011

Thosar, S. S., Butler, M. P., & Shea, S. A. (2018). Role of the circadian system in cardiovascular disease. *Journal of Clinical Investigation*, *128*(6), 2157–2167. https://doi.org/10.1172/JCI80590

Tian, R., Colucci, W. S., Arany, Z., Bachschmid, M. M., Ballinger, S. W., Boudina, S., Bruce, J. E., Busija, D. W., Dikalov, S., Dorn, G. W., Galis, Z. S., Gottlieb, R. A., Kelly, D. P., Kitsis, R. N., Kohr, M. J., Levy, D., Lewandowski, E. D., McClung, J. M., Mochly-Rosen, D., … Shi, S. (2019). Unlocking the Secrets of Mitochondria in the Cardiovascular System. *Circulation*, *140*(14), 1205–1216. https://doi.org/10.1161/CIRCULATIONAHA.119.040551

Van Heerebeek, L., & Paulus, W. J. (2016). Understanding heart failure with preserved ejection fraction: Where are we today? *Netherlands Heart Journal*, *24*(4), 227–236. https://doi.org/10.1007/s12471-016-0810-1

Wang, W., Yuan, R. K., Mitchell, J. F., Zitting, K.-M., St. Hilaire, M. A., Wyatt, J. K., Scheer, F. A. J. L., Wright, K. P., Brown, E. N., Ronda, J. M., Klerman, E. B., Duffy, J. F., Dijk, D.-

J., & Czeisler, C. A. (2023). Desynchronizing the sleep-–wake cycle from circadian timing to assess their separate contributions to physiology and behaviour and to estimate intrinsic circadian period. *Nature Protocols*, *18*(2), 579–603. https://doi.org/10.1038/s41596-022-00746-y

Wei, C., Li, D., Zhang, M., Zhao, Y., Liu, Y., Fan, Y., Wang, L., Liu, J., Chang, X., Jiang, Y., & Xiong, H. (2024). Prevalence of Adeno-Associated Virus-9-Neutralizing Antibody in Chinese Patients with Duchenne Muscular Dystrophy. *Human Gene Therapy*, *35*(1–2), 26–35. https://doi.org/10.1089/hum.2023.117

Wei, S., Guo, A., Chen, B., Kutschke, W., Xie, Y.-P., Zimmerman, K., Weiss, R. M., Anderson, M. E., Cheng, H., & Song, L.-S. (2010). T-Tubule Remodeling During Transition From Hypertrophy to Heart Failure. *Circulation Research*, *107*(4), 520–531. https://doi.org/10.1161/CIRCRESAHA.109.212324

When are mice considered old? (n.d.). The Jackson Laboratory. Retrieved May 8, 2024, from https://www.jax.org/news-and-insights/jax-blog/2017/november/when-are-mice-considered-old

Xing, S., Tsaih, S.-W., Yuan, R., Svenson, K. L., Jorgenson, L. M., So, M., Paigen, B. J., & Korstanje, R. (2009). Genetic influence on electrocardiogram time intervals and heart rate in aging mice. *American Journal of Physiology - Heart and Circulatory Physiology*, *296*(6), H1907–H1913. https://doi.org/10.1152/ajpheart.00681.2008

Yan, T., Zhu, S., Yin, X., Xie, C., Xue, J., Zhu, M., Weng, F., Zhu, S., Xiang, B., Zhou, X., Liu, G., Ming, Y., Zhu, K., Wang, C., & Guo, C. (2023). Burden, Trends, and Inequalities of

Heart Failure Globally, 1990 to 2019: A Secondary Analysis Based on the Global Burden of Disease 2019 Study. *Journal of the American Heart Association*, *12*(6), e027852. https://doi.org/10.1161/JAHA.122.027852

Young, M. E., Brewer, R. A., Peliciari-Garcia, R. A., Collins, H. E., He, L., Birky, T. L., Peden, B. W., Thompson, E. G., Ammons, B.-J., Bray, M. S., Chatham, J. C., Wende, A. R., Yang, Q., Chow, C.-W., Martino, T. A., & Gamble, K. L. (2014). Cardiomyocyte-Specific BMAL1 Plays Critical Roles in Metabolism, Signaling, and Maintenance of Contractile Function of the Heart. *Journal of Biological Rhythms*, *29*(4), 257–276. https://doi.org/10.1177/0748730414543141

Zheng, Y., Pan, L., Wang, F., Yan, J., Wang, T., Xia, Y., Yao, L., Deng, K., Zheng, Y., Xia, X., Su, Z., Chen, H., Lin, J., Ding, Z., Zhang, K., Zhang, M., & Chen, Y. (2023). Neural function of Bmal1: An overview. *Cell & Bioscience*, *13*(1), 1. https://doi.org/10.1186/s13578-022-00947-8